ChemMedChem

Research Article
doi.org/10.1002/cmdc.202300109

Chemistry Europe
European Chemical Societies Publishing

www.chemmedchem.org

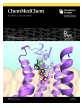

Are Two Riboses Better Than One? The Case of the Recognition and Activation of Adenosine Receptors

Teresa Gianferrara,[a] Matteo Pavan,[b] Davide Bassani,[b] Fabrizio Vincenzi,[c] Silvia Pasquini,[d] Giovanni Bolcato,[b] Katia Varani,[c] Giampiero Spalluto,[a] Stephanie Federico,[a] and Stefano Moro*[b]

Traditionally, molecular recognition between the orthosteric site of adenosine receptors and their endogenous ligand occurs with a 1:1 stoichiometry. Inspired by previous mechanistic insights derived from supervised molecular dynamics (SuMD) simulations, which suggested an alternative 2:1 binding stoichiometry, we synthesized BRA1, a bis-ribosyl adenosine derivative, tested its ability to bind to and activate members of the adenosine receptor family, and rationalized its activity through molecular modeling.

Introduction

At the end of the 19th century, Paul Ehrlich stated a quote that would mark a decisive moment in the history of biochemistry, other than becoming a pillar of the modern drug discovery process: "Corpora non agunt nisi fixata".[1] These words summarize the principle by which, to produce a biological response, any molecule has to bind with a partner within the organism. The large variety of subfamilies for both ligands (e.g., small molecules, peptides, antibodies, aptamers, etc.) and their biological partners (e.g., proteins and nucleic acids) provides a complex interaction landscape through which Mother Nature establishes its intricate balance.

The study of the response obtained when a ligand approaches a target biomolecule has allowed the scientific community to further increase the complexity of the topic by distinguishing various mechanisms of action, including full agonism, antagonism, partial agonism, and inverse agonism.[2] A crucial piece of the protein-ligand recognition puzzle was later added with the observation that a molecule could bind to the same target at multiple sites and that different sites on the same macromolecule could elicit different biological responses. From that moment on, orthosteric binders were distinguished from allosteric ones.[3]

Another aspect that emerged from the mechanistic studies concerns the stoichiometry by which the recognition process takes place. Although the most common scenario is for a single ligand molecule to interact with a single receptor molecule, there are many exceptions to this rule to date. In this regard, the endogenous neurotransmitter acetylcholine is, perhaps, the most remarkable example of an alternative binding stoichiometry to canonical 1:1, recognizing its nicotinic receptors in a 2:1 ratio to produce the associated biological response.[4]

As for the orthosteric ligands, the 1:1 stoichiometry rule still undisputedly reigns in many fields of drug discovery, and one of these is certainly associated with G protein-coupled receptors (GPCRs). To date, this family consists of more than 800 members, and is one of the most populated protein families in the human organism, making them a very popular class of targets in drug discovery campaigns.[5] From a topological and structural point of view, these receptors are embedded in the cellular membrane and consist of an N-terminal (N-ter) extracellular and an intracellular C-terminal (C-ter) domain, between which lies a transmembrane region formed by seven α-helices (also called 7TM domain). These helices are joined by six different loops, three of which are located on the extracellular side of the membrane (extracellular loops, or ECLs), while the other three lie on the intracellular one (intracellular loops or ICLs).[6]

The allosteric modulators of these proteins are well known,[7] and in many cases have still made their way through the drug discovery pipeline to the market,[8] once again re-establishing the principle that multiple molecular entities can bind to different portions of the receptor and cooperate in modulating their biological response. On the contrary, the possibility for these proteins to allocate two different molecules

[a] Prof. T. Gianferrara, Prof. G. Spalluto, Prof. S. Federico
Department of Chemical and Pharmaceutical Sciences
University of Trieste
Via Licio Giorgieri 1, 34127 Trieste (Italy)
[b] M. Pavan, D. Bassani, G. Bolcato, Prof. S. Moro
Molecular Modeling Section (MMS)
Department of Pharmaceutical and Pharmacological Sciences
University of Padova
Via Francesco Marzolo 5, 35131 Padova (Italy)
E-mail: stefano.moro@unipd.it
[c] Prof. F. Vincenzi, Prof. K. Varani
Department of Translational Medicine
University of Ferrara
Via Luigi Borsari 46, 44121 Ferrara (Italy)
[d] Dr. S. Pasquini
Department of Chemical and Agricultural Sciences
University of Ferrara
Via Luigi Borsari 46, 44121 Ferrara (Italy)

Supporting information for this article is available on the WWW under https://doi.org/10.1002/cmdc.202300109

in the same orthosteric binding site has never been experimentally proven.

A prospective computational study by Deganutti et al.[9] speculated that it would be possible for the adenosine receptor A2 A to simultaneously host two different adenosine molecules in the orthosteric binding site. By exploiting Supervised Molecular Dynamics simulations (SuMD),[10] Deganutti et al. proposed three different possible states for the 2:1 adenosine-receptor complex, each of them depicting the key interactions by which the endogenous ligand exerts its activity. Despite the intriguing insights provided by this computational investigation, so far the resulting hypothesis about an alternative binding stoichiometry has never been proven experimentally, mainly due to the level of complexity that the test required for this task would imply. Adenosine is rapidly both metabolized and formed in biological preparations including membrane preparations that are those generally used in binding assays, thus reliable data cannot be obtained.

To avoid these limitations and experimentally support the hypothesis of an alternative adenosine binding stoichiometry to the canonical 1:1, we synthesized a bis-ribosyl adenosine derivative (N6-(D-ribos-1-yl)-adenosine / BRA1, chemical structure reported in Figure 1) and tested its ability to bind to and activate the members of the adenosine receptors family.

In this scientific work, we used BRA1 as a probe compound to validate the capability of the orthosteric site of the adenosine receptors to contemporarily host two different adenosine molecules at the same time, without hampering the receptor activation process. In particular, we used a combined experimental and computational approach to determine the activity and selectivity profile of this bis-ribosyl compound and characterize its mechanism of action by investigating its ability to recognize the orthosteric site of adenosine receptors A1, A2 A, and A3. Due to the presence of the solution equilibrium between the five different isomer species of the N6-(D-ribos-1-yl)-adenosine compound, in our computational study we considered them as separated entities, to independently evaluate their ability to contribute to the activity of the ligand. Through this work, we hope to broaden the knowledge of GPCR ligand recognition and guide the development of novel active molecules that could exploit hitherto unexplored non-canonical interaction patterns.

Results and Discussion

Chemistry

An attempt to synthesize N6-(D-ribos-1-yl)-adenosine was reported in 1968 by reacting 2–3-5-tri-O-benzoyladenosine and 1′-O-acetyl-2′-3′-5′-tri-O-benzoyl-D-ribofuranose at solid-state at 140 °C in the presence of anhydrous zinc chloride, followed by debenzoylation of the protected diriboside with a catalytic amount of sodium methoxide.[24] The final product was characterized only utilizing UV-visible spectroscopy and elemental analysis. To the best of our knowledge, no more recent attempt to synthesize this nucleoside derivative is reported in the literature. Recently, Gates and coworkers described a one-step synthesis of N6-(2-deoxy-D-ribos-1-yl)-2′-deoxyadenosine by reacting 2′-deoxyadenosine and 2-deoxyribose in an acidic medium (at 37 °C for 72 h).[25] To accomplish a reliable synthesis of N6-(D-ribos-1-yl)-adenosine, we performed the acid-catalyzed reaction with the microwave-assisted approach. The substrates adenosine and D-(−)-ribose were suspended in methanol and glacial acetic acid (7:3), and heated in a microwave oven at 100 °C (power 850 W) for 60 min. The resulting solution was evaporated to dryness and purified by column chromatography on silica gel. The pure product was isolated as a very hygroscopic white solid in good yield (60 %) and fully characterized by proton NMR and 2D NMR experiments (COSY, HSQC, and TOCSY), ESI-MS spectrometry, HPLC and LC/MS analysis.

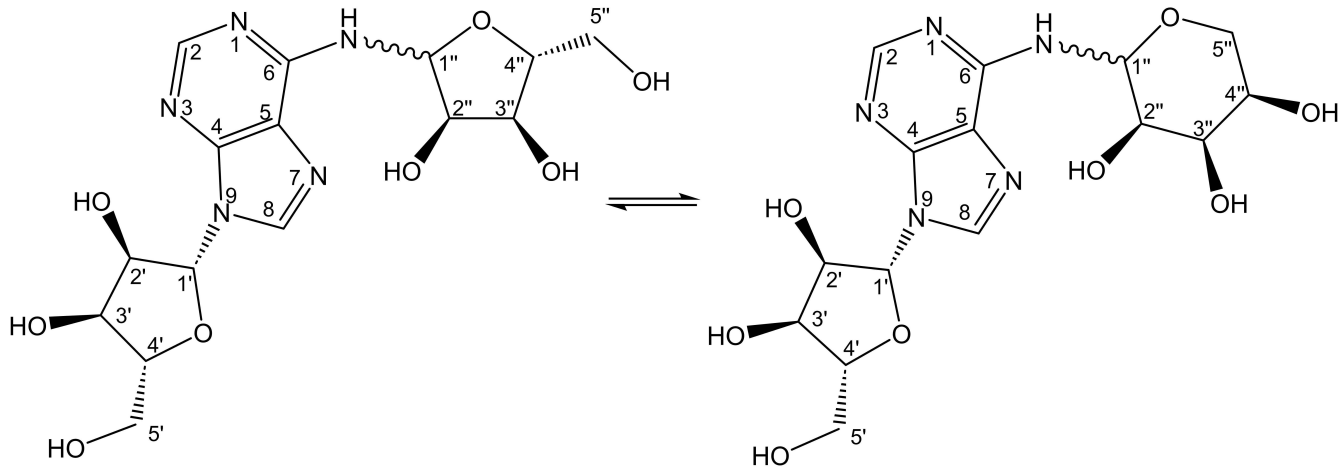

Figure 1. Representation of the solution equilibrium between the ribofuranose and ribopyranose form of the N6-(D-ribos-1-yl)-adenosine (BRA1) compound synthesized and evaluated in this study. Each isomer can have two different anomeric forms, α, and β, which leads to a total of four different solution species of the same compounds. The open-ring form is also present, but its relative solution concentration is negligible and, for this reason, it is not considered in this study (see Supporting Information).

According to the reaction mechanism (Figure 2A) and in agreement with the literature,[26] the adduct N6-(D-ribos-1-yl)-adenosine is present in solution as an equilibrium mixture of the α-pyranose (α-PYR), β-pyranose (β-PYR), α-furanose (α-FUR), and β-furanose (β-FUR) isomers (Figure 1). The proton NMR spectrum of N6-(D-ribos-1-yl)-adenosine (Supporting Information, Figure S1) recorded in D2O at T = 40 °C showed in the upfield region the resonances of the D-ribose unit connected to the N9-amino group of adenine. A TOCSY spectrum confirmed the presence of the proton-proton spin system H1′-H5′ of the N9-ribose (Supporting Information, Figure S2). As expected, the region of the anomeric proton H1″ of the N6-linked ribose showed multiple resonances between 5.5-6.3 ppm (Figure 2B), and the analysis of the TOCSY experiment revealed four different proton-proton spin systems H1″-H5″ (Supporting Information, Figure S3), reflecting the isomeric composition in solution. In the HSQC spectrum the four resonances of the protons H1″ correlate with C1″ atoms at 81.6, 85.1, 78.6, and 78.1 ppm (Supporting Information, Figure S4), thus suggesting that the isomers are cyclic structures and no acyclic form is present in the equilibrium mixture. The two anomeric C1″ that resonate at lower fields belong to 5-member ring, while the two higher-field resonances have been attributed to 6-member ring. This attribution is consistent with the results of a 13 C NMR study on N-phenyl-D-ribosylamines where the value of the chemical shift of the anomeric carbon C1″ allowed to identify of the furanoid and the pyranoid form since a carbon resonates at lower fields in a 5-term cycle than in a 6-term cycle.[27] Based on the integration of the resonances of H1″ protons, the ratio between pyranoid and furanoid isomers in D2O was ~90:10 (Figure 2B), in agreement with the predomination of α- and β-pyranose isomers observed both for ribose[28,29] and for N-aryl-aminoribose derivatives.[27,30–32]

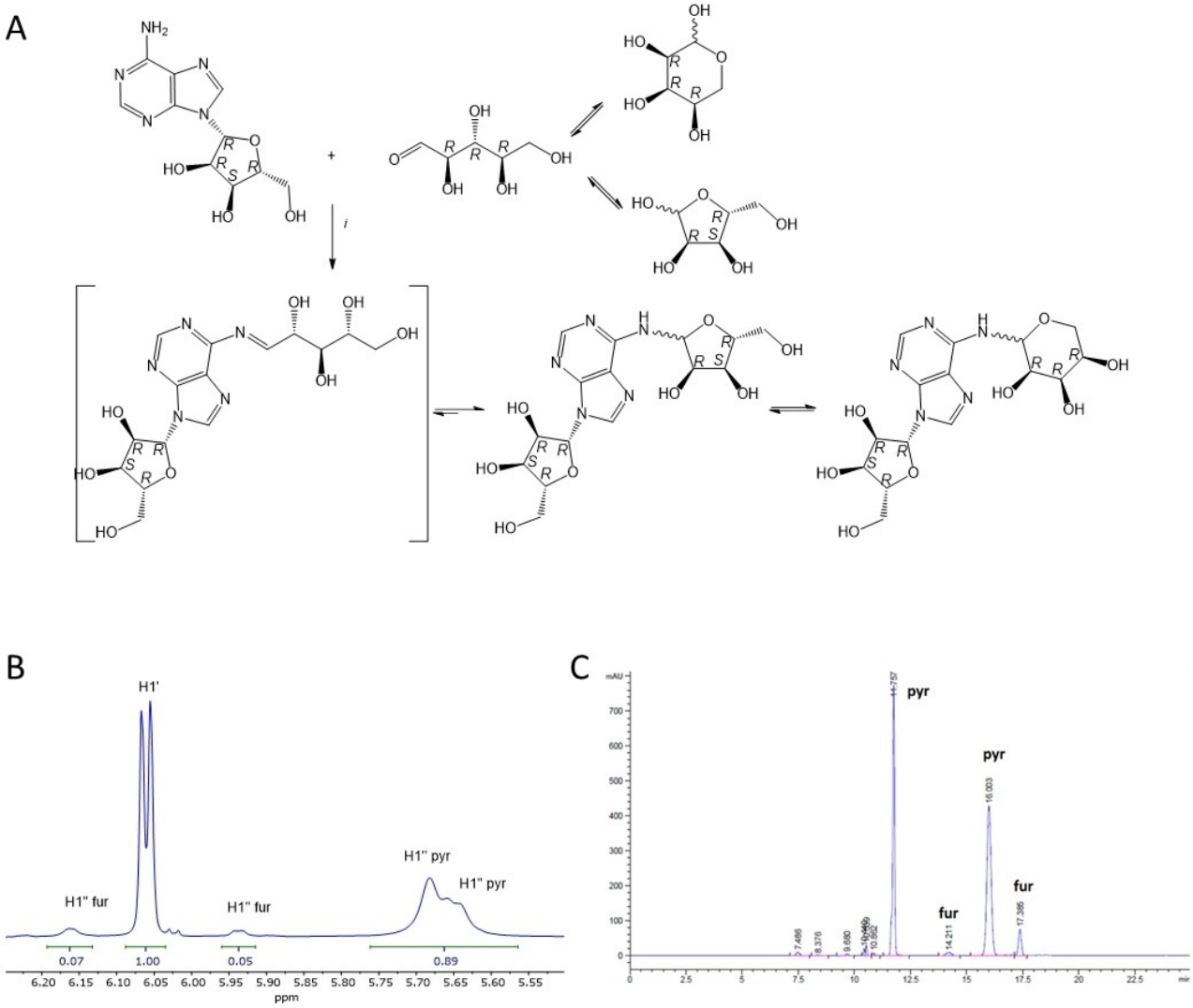

Figure 2. A) Schematic synthesis of N6-(D-ribos-1-yl)-adenosine. i: anhydrous methanol (700 μL), glacial acetic acid (300 μL), MW irradiation 60 min at 100 °C, power 850 W, stirrer speed 800 rpm; yield 60%. B) 1H NMR spectrum of N6-(D-ribos-1-yl)-adenosine in D2O at T = 40 °C in the region of the anomeric protons H1′ and H1″; see Figure 1 for numbering scheme. C) HPLC chromatogram of pure N6-(D-ribos-1-yl)-adenosine. The peaks of the major pyranoid (pyr) and the minor furanoid (fur) isomers are labeled. See Experimental protocol for the detailed separation conditions.

The α and β-isomers are separable by HPLC using water and a small percentage of acetonitrile as mobile phase (Figure 2C), and the purity of the compound BRA1 was found to be 96%. Based on the integration areas, the ratio between the two pyranoid and furanoid isomers was 90: 10 in agreement with the NMR data. Furthermore, the LC/MS analysis of the same sample revealed four isomers with virtually identical ESI-MS spectra (Supporting Information, Figures S5-S7). The total purity of the sample evaluated based on the LC/MS chromatogram at λ 250.8 nm is 95% and is in very good agreement with the 96% value of the HPLC analysis.

Pharmacology

BRA1 was tested for its affinity at hA1, hA2 A, and hA3 ARs stably transfected in CHO cells. The compound showed Ki values in the micromolar range, showing a higher affinity (in the low micromolar range) to A1ARs and a lower one (in the mid-micromolar range) to A2 A and A3 ARs (Table 1, Figure 3A). Moreover, BRA1 was examined in the cAMP assay to assess its capability to modulate cAMP level production. The compound, evaluated in the presence (for A1 and A3 ARs) or in the absence (for A2 A and A2B ARs) of 1 μM forskolin, resulted in a full, transfer micromolar affinity one micromolar potency it agonist to ARs. Accordingly, BRA1 showed potency in the low micromolar range for A1ARs and the mid-micromolar range for the

Table 1. Summary of pharmacological results.

Competition binding experiments	A_1ARs [^{3}H]CCPA K_i [μM]	A_{2A}ARs [^{3}H]ZM241385 K_i [μM]	A_{2A}ARs [^{3}H]CGS 21680 K_i [μM]	A_3ARs [^{125}I]ABMECA K_i [μM]
BRA1	3.15 ± 0.21	45 ± 4	95 ± 9	84 ± 7
cAMP experiments	**A_1ARs IC_{50} [μM]**	**A_{2A}ARs EC_{50} [μM]**	**A_{2B}ARs EC_{50} [μM]**	**A_3ARs IC_{50} [μM]**
BRA1 (full agonist)	1.02 ± 0.17	103 ± 8	590 ± 55	350 ± 32
Adenosine[a]	0.31	0.73	23.5	0.29

[a] Data from Ref. [32].

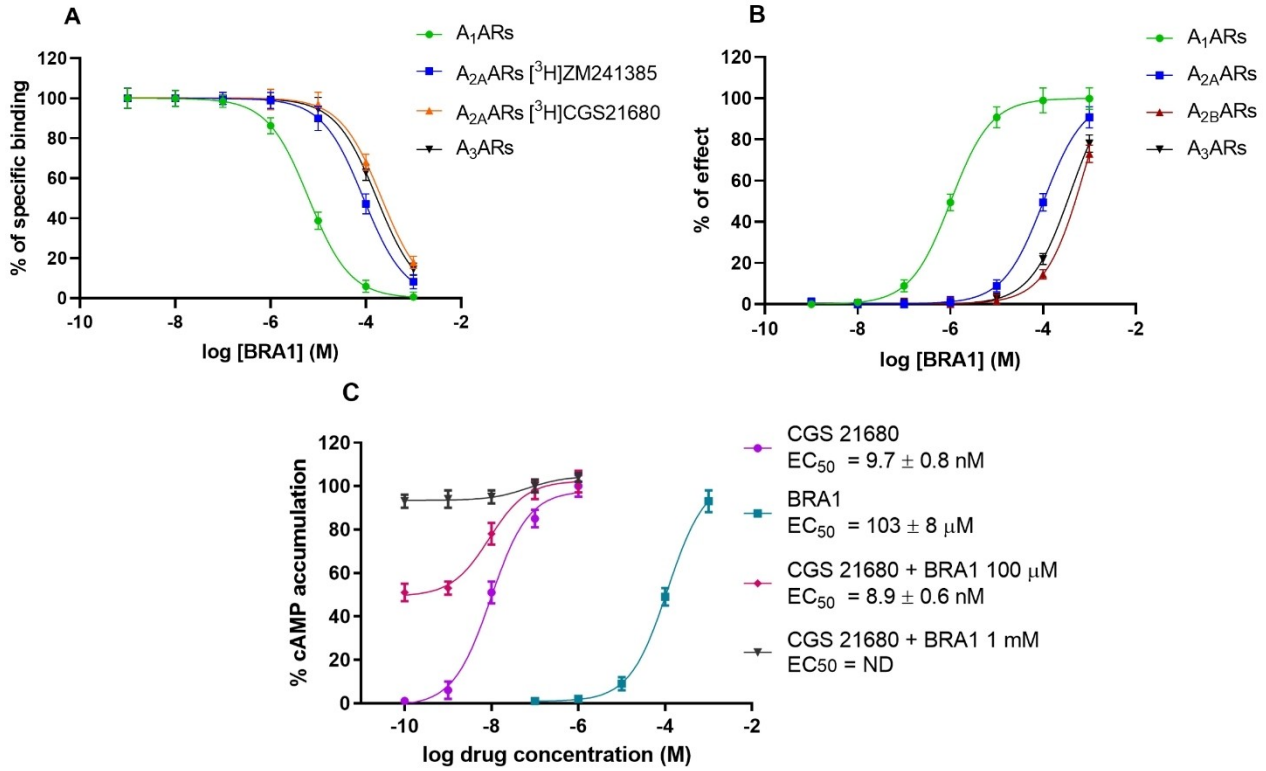

Figure 3. A) Competition curves of specific binding to hA1, hA2 A, and hA3 ARs of BRA1. B) Concentration-response curves of BRA1 on cAMP modulation. In cAMP assays performed in CHO cells transfected with hA1 and hA3 ARs, BRA1 reduced forskolin-stimulated cAMP accumulation. In cAMP experiments performed in CHO cells transfected with hA2 A and hA2B ARs, BRA1 induced an increase in cAMP production. C) Concentration-response curves of CGS21680 and BRA1 on cAMP modulation in CHO cells transfected with hA2 A. ND = not determinable.

other AR subtypes (Table 1, Figure 3B). Additional evidence of BRA1-mediated full agonism comes from its effect on CGS 21680-mediated activation of A2 A AR. Figure 3, panel C shows that the addition of a fixed concentration of BRA1 did not change the EC50 value of CGS 21680, thus it is not an allosteric modulator of the receptor, while basal cAMP levels raised with the increase of BRA1 concentration, behaving additive to CGS 21680 in activating the receptor (Figure 3C).

Computational evaluation

To computationally evaluate how the synthetic bis-ribosyl derivative BRA1 would bind each adenosine receptor orthosteric site, docking calculations were carried out for each of the four prevalent solution species of N6-(D-ribos-1-yl)-adenosine, α-FUR, β-FUR, α-PYR, β-PYR respectively, against each considered adenosine receptor subtype A1, A2 A, and A3. The experimentally solved structures for adenosine receptors A1 and A2 A were available on the Protein Data Bank (PDB), with accession codes 6D9H and 2YDO respectively. These two structures were chosen, among the available ones, since they are complexed with the endogenous agonist adenosine, which is the starting point for the development of the BRA1 ligand and is, therefore, the point of reference for structural evaluations and the comparison of binding features. On the contrary, no experimentally solved structures were available for the A3 receptor, therefore a homology model based on the A1 structure (PDB ID: 6D9H), was built and utilized for docking calculations. Finally, since the experimental structure of the adenosine receptor A2B in complex with adenosine was recently solved (PDB ID: 8HDP), we also hypothesized how would BRA1 bind to A2B orthosteric site.

Adenosine A1 receptor

Docking calculations results and subsequent analysis for the A1 adenosine receptor are summarized in Figure 4 and Figure 5, which report a per-residue decomposition of the protein-ligand

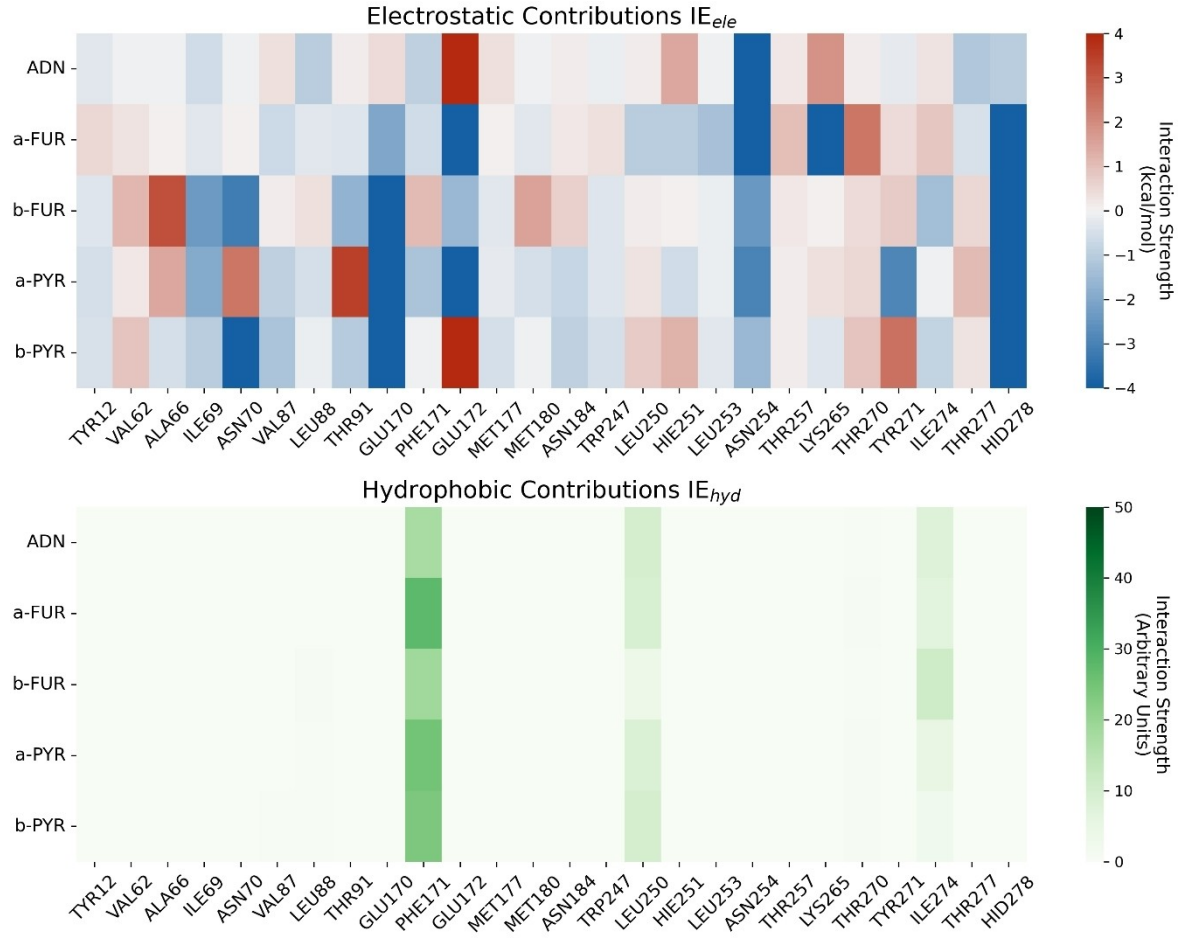

Figure 4. Per-residue interaction energy heatmap encompassing the recognition features of the best docking pose for each of the four solution species of N6-(D-ribos-1-yl)-adenosine and for the crystal adenosine within the orthosteric binding site of adenosine receptor A1 (PDB ID: 6D9H). The vertical axis reports the compound name, while the horizontal axis reports the protein residue name. The upper plot depicts a per-residue decomposition of the electrostatic interaction energy, with colors ranging from blue (negative, thus attractive, interaction energy value) to red (positive, therefore repulsive, interaction energy value). The lower plot, instead, illustrates a per-residue decomposition of the hydrophobic interaction contribution to the total interaction energy, ranging from white (low intensity) to dark green (high intensity).

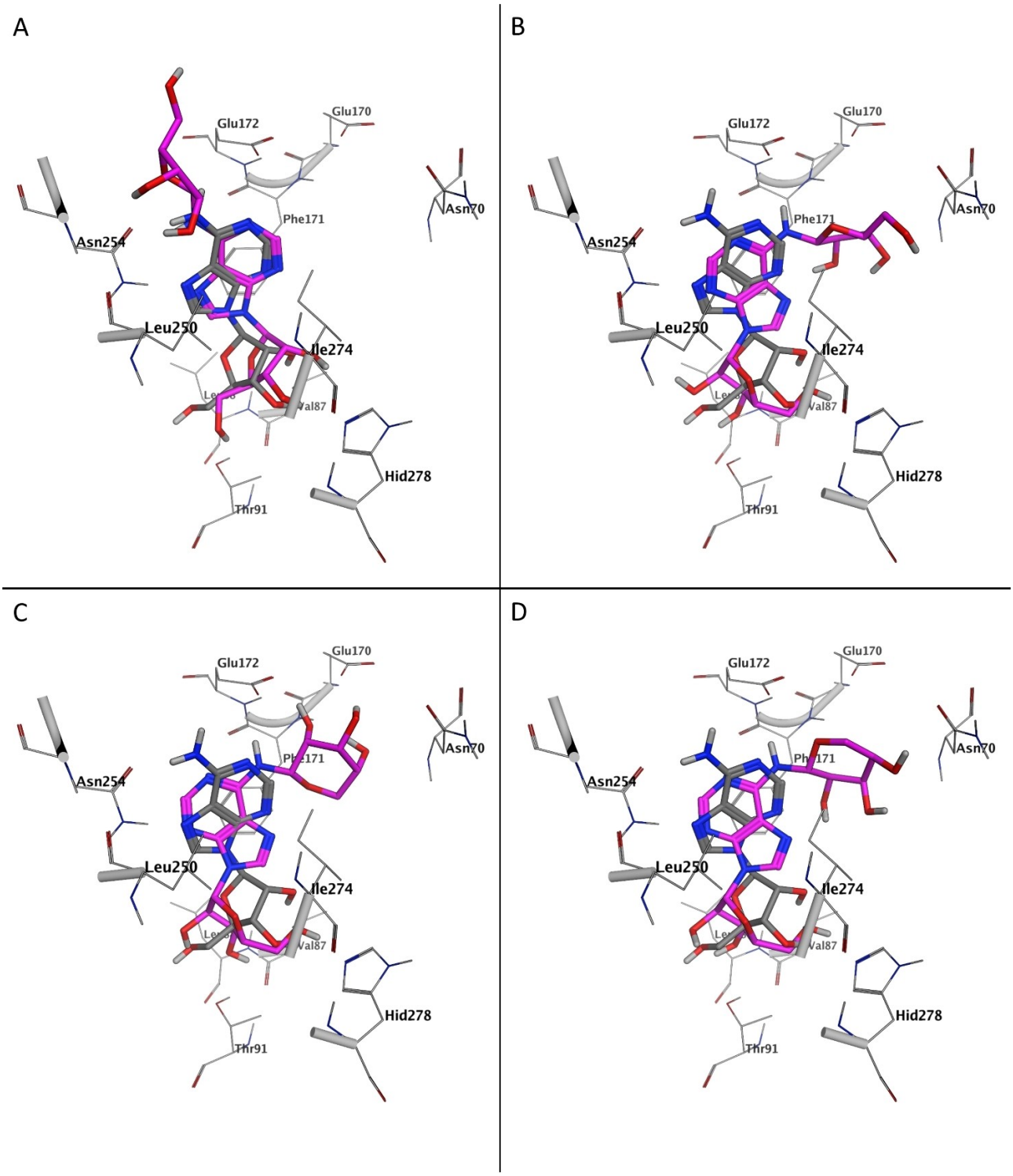

Figure 5. This panel reports the superposition of the best docking pose within the orthosteric binding site of the A1 adenosine receptor for each of the four solution species of N6-(D-ribos-1-yl)-adenosine (magenta) and the crystal pose of adenosine (grey). A) α-FUR. B) β-FUR. C) α-PYR. D) β-PYR.

interaction energy and a superposition between the crystal binding mode for the endogenous ligand adenosine and the best docking pose for each solution species of BRA1, respectively, as well as in Video_S1 (Supporting Information). As can be seen in both Figure 5 (panel A) and Figure 4, the highest degree of congruence between the docking-predicted binding mode for one of the isomeric forms of BRA1 and the crystal adenosine is obtained in the case of α-FUR. Particularly, α-FUR can preserve the full interaction pattern of the adenosine scaffold (the double hydrogen bond between the adenine

moiety and the Asn254 sidechain, the π-stacking between the adenine portion and Phe171), as found in the reference crystal structure, while adding some additional interactions features with residues located in the upper portion of the binding site, such as Glu170 and Glu172, as highlighted by the per-residue heatmap reported in Figure 4. Despite not reaching such a high level of agreement between the reference binding mode and the query docking pose, even other solution species are predicted to form bound complexes that preserve most, if not the totality, of intermolecular interactions that are required for the binding of adenosine. Peculiarly, each isomer can form at least one hydrogen bond between the adenine moiety and the Asn254 sidechain, despite an overall different orientation of this fraction of the ligand within the binding site compared to the crystal reference. Moreover, the change in the orientation of the adenine portion does not interfere with the formation of a π-stacking interaction with the sidechain of Phe171. All things considered, it seems that the synthetic bis-ribosyl derivative can bind the orthosteric binding site of adenosine receptor A1 with an interaction pattern that is practically superimposable to one of the endogenous ligand adenosine. That is especially true in the case of the α-FUR isomer, but the presence of a sub-optimal recognition pattern also for the other solution species of BRA1 leads to the hypothesis that the binding event might not be exclusive to the best fitting isomer, especially considering that the pyranoid isomers are the predominant species in solution (Figure 2). Interestingly, a glance at the predicted interaction pattern with other adenosine receptor subtypes reveals that the α-FUR–A1 complex is the only case in which the canonical adenosine binding mode involving the double hydrogen bond between the adenine moiety and the sidechain of the asparagine residue located on the sixth transmembrane helix (Asn254, in the case of A1) is maintained. This could be a possible explanation for the higher binding affinity of N6-(D-ribos-1-yl)-adenosine for the A1 adenosine receptor compared to other subtypes (Table 1).

Adenosine A_{2A}, A_3 and A_{2B} receptors

As for receptor A1, the results of docking calculation and subsequent analysis for the A2 A and A3 adenosine receptors are summarized in Figure S10-S11 and Figures 6 and 7, as well as in Video_S2 and Video_S3 (Supporting Information). Coherently with the lower affinity value for BRA1 for these two receptor subtypes compared to A1, none of the docking poses produced for the query compound N6-(D-ribos-1-yl)-adenosine exactly matches the atomic disposition within the orthosteric binding site of adenosine. Despite this, as can be seen in Figure S10, the interaction pattern is prevalently conserved, especially the π-stacking with Phe168, electrostatic interactions that involve the N9-linked ribose unit, and residues in the lower part of the binding site such as Thr88, Ser277, and His278 (which are flagged as crucial for the receptor activation process). Compared to the crystal adenosine, the interaction with Asn253 is not as well maintained as in the case of the A1 receptor due to the alternative orientation of the adenine moiety that serves to better accommodate the N6-linked ribose unit within the upper portion of the binding site. The loosening of this interaction seems to be compensated by the strengthening of other auxiliary interactions with residues such as Leu167, Phe168, His250, and Ile274. Notably, the hydrogen bond between the exocyclic amine group of the adenine core of adenosine and the sidechain of Glu169 is replaced by analogous interactions portrayed by the N6-linked ribose unit. Curiously, the interaction pattern of α-FUR closely recalls the one that was recently described by Supervised Molecular Dynamics (SuMD) simulations for the non-ribose agonist LUF5833:[34] as described in the original publication, the non-ribose agonist can replace the required ribose-involving interactions by stabilizing a network of water molecules. Despite the obvious difference in the ability to interact with the lower part of the binding site due to the lack/presence of the ribose moiety, the rest of the defining interaction features are practically superimposable, especially the lower importance of the interaction with Asn253 in stabilizing the bound complex. Concerning this, it is tempting to speculate that the presence of a secondary ribose unit attached to the adenine core of adenosine renders the ligand more similar to a non-ribose agonist rather than to the starting molecule. A thorough investigation of this hypothesis through the exploitation of SuMD simulations and algorithms which track the behavior of water molecules such as AquaMMapS,[35] as successfully applied in the work of Bolcato et al.,[34] is already going on within our laboratory and will be part of future scientific works. Notably, the observations about the binding pattern predicted for the α-FUR are also in agreement with the work of Deganutti et al.,[9] where the stabilization of the secondary adenosine molecule within the orthosteric binding site coincided with a partial loss of interaction between the protein and the already-bound adenosine mainly caused by the loss of hydrogen bonds with the sidechain of Asn253. Furthermore, the interaction of the N6-linked ribose unit with the sidechain of Glu169 closely recalls the orientation and the binding determinants of the extracellular adenosine molecule in the ribose up conformation, especially concerning the bound state B and E described in the original publication. The striking similarities between the binding determinants predicted for the ternary complex by Supervised Molecular Dynamics simulations and the one predicted by docking for the bis-ribosyl adenosine derivative not only strengthen the possibility of a 2:1 binding stoichiometry for adenosine in the case of A2 A but also extends this possibility to other adenosine receptor subtypes, particularly A1 which is the only case which presents a docking pose for BRA1 which perfectly matches the experimental binding mode for adenosine and is, indeed, the one which presents the highest binding affinity for BRA1. Concerning the difference between the four solution species of BRA1, once again the comparison between the interaction pattern of crystal adenosine and each isomer once again indicates α-FUR as the one that most closely resembles the interaction pattern of crystal adenosine. The observation that, for both A1 and A2 A, the favored isomer is the one with two ribose units in the furanoid configuration is also a further indication of a possible 2:1 binding stoichiometry,

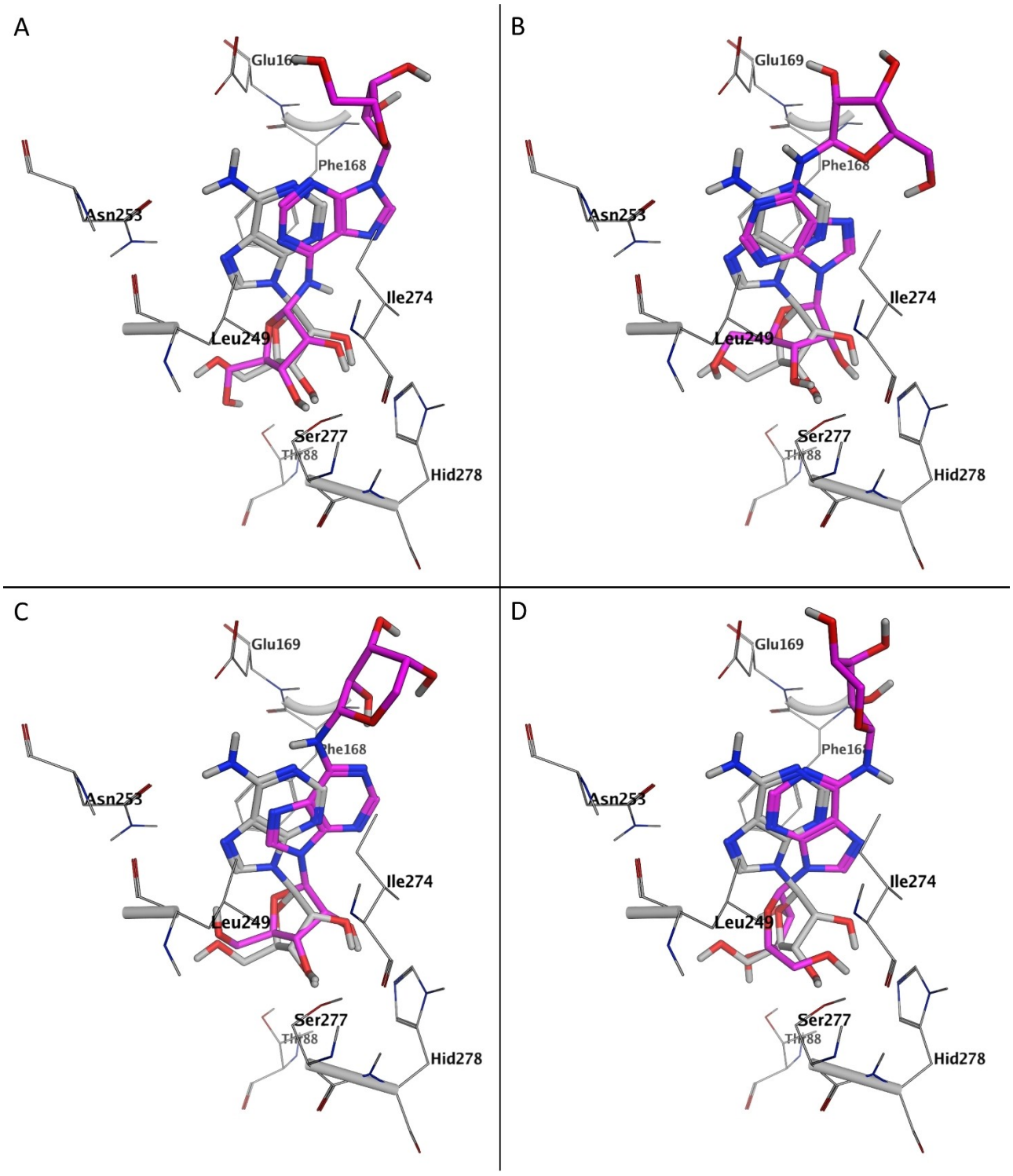

Figure 6. This panel reports the superposition of the best docking pose within the orthosteric binding site of the A2 A adenosine receptor for each of the four solution species of N6-(D-ribos-1-yl)-adenosine (magenta) and the crystal pose of adenosine (grey). A) α-FUR. B) β-FUR. C) α-PYR. D) β-PYR.

with the ribose down adenosine binding first and establishing favorable interactions with the lower portion of the binding site which are needed for the receptor activation and the second, ribose up, adenosine molecule subsequently binding, providing the additional interactions with the upper part of the binding site (similarly to the N6-linked ribose unit in the BRA1 compound) and therefore leading to the stabilization of the ternary complex.

Accordingly, the analysis of the predicted interaction pattern for the various solution species of BRA1 against A3 is similar to what was already described for receptors A1 and A2 A, with the α-FUR isomer being able to replicate the binding

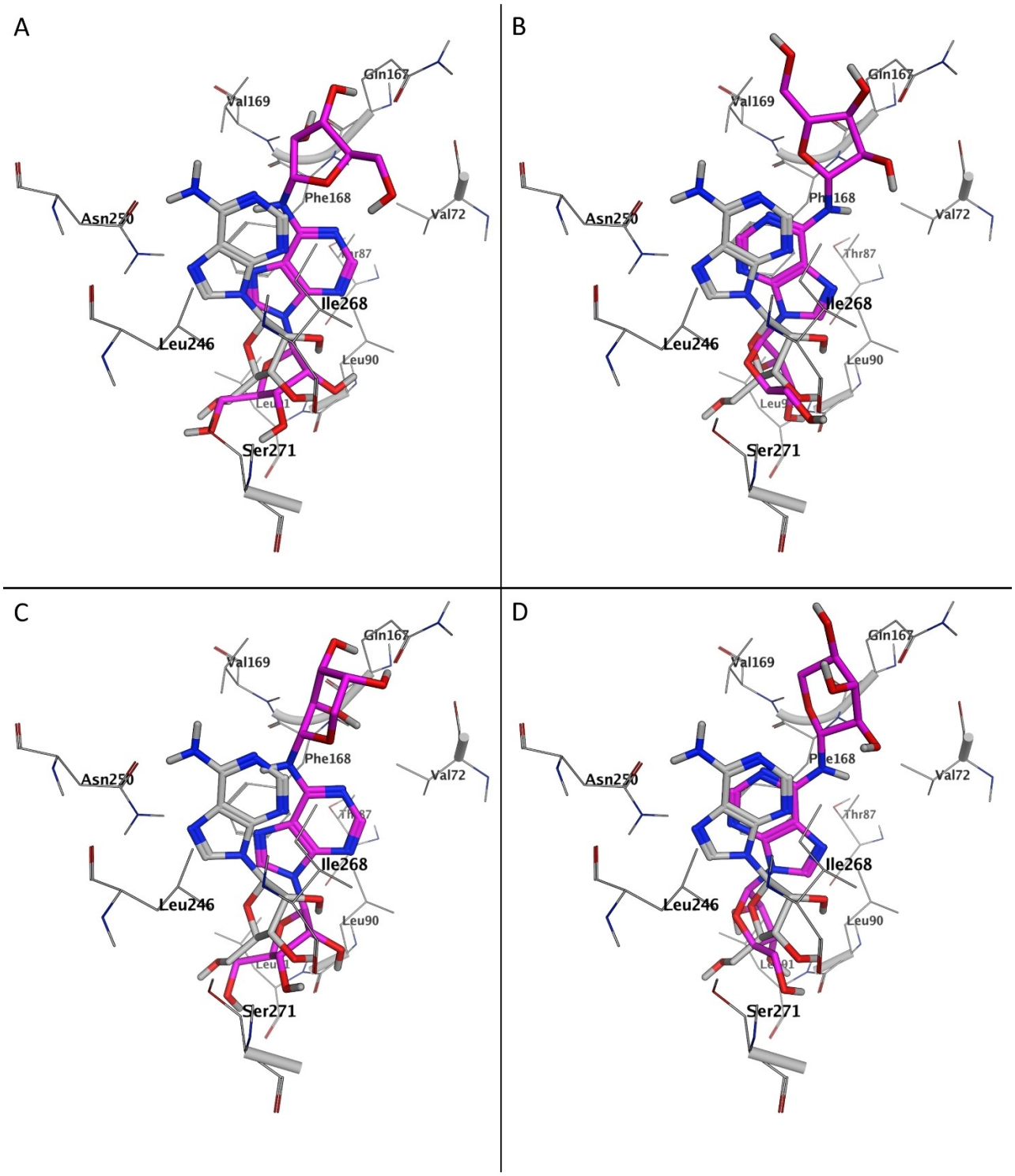

Figure 7. This panel reports the superposition of the best docking pose within the orthosteric binding site of the A3 adenosine receptor for each of the four solution species of N6-(D-ribos-1-yl)-adenosine (magenta) and the reference binding pose of adenosine (grey). A) α-FUR. B) β-FUR. C) α-PYR. D) β-PYR.

determinants of adenosine quite well, except for the double hydrogen bond with Asn250. As anticipated in the case of adenosine receptor A2 A, the absence of a pose that exactly matches the recognition pattern for the endogenous adenosine could be a possible explanation for the lower affinity of the BRA1 for receptor subtypes A2 A and A3 compared to A1 (Table 1). Despite the lack of this double hydrogen bond interaction with the asparagine sidechain, which is pivotal to the recognition of adenosine, the rest of the intermolecular binding features are retained and even strengthened. Intrigu-

ingly, favorable contacts involve residues such as Val65, Val72, Ser73, Thr87, Thr94, Asn250, Gln261, and Ser271, other than a triplet of residues (Gln167, Phe168, and Val169) located on the ECL2 which lines the upper portion of the binding site (Figure S11). Notably, BRA1 can establish favorable electrostatic interactions with the sidechain of the residue that precedes the crucial phenylalanine responsible for the π-stacking with the aromatic adenine core, Gln167 in this case. It is interesting to notice how the aminoacidic composition of this upper portion of the binding site, particularly regarding the residue i-1 and i+1 relative to the position of the crucial phenylalanine residue, plays a pivotal role in determining the orientation and the binding features of the N6-linked ribose unit. This change in the aminoacidic composition of this receptor region, could not only be crucial in the stabilization of the bound complex but would probably be the protagonist at an earlier stage, while the ligand approaches the binding site. This is not surprising, considering that the pivotal role of ECL2 in steering the binding event is well renowned and characterized in the world of GPCR.[36] Limiting the discussion to the role of this vestibular region in the binding affinity for the BRA1 ligand, it seems that the polarity and charge properties of the residues surrounding the crucial phenylalanine residue are pivotal in establishing intermolecular interactions with the N6-linked ribose unit, in particular, related to hydrogen bonds between the sidechain of those residues and the hydroxyl groups of the ribose. If that is the case, this could be an additional explanation (other than the quality of interaction with the sidechain of asparagine residue) for the lower binding affinity of BRA1 for receptors A2 A and A3 compared to A1: indeed, while A1 presents two charged amino acids surrounding the phenylalanine residue (Glu170 and Glu172, respectively), A2 A only presents one charged residue (Glu169) with the other residue being hydrophobic (Leu167) and A3 do not present any charged amino acids, with the i-1 and i+1 residues being Gln167 and Val169, respectively.

Finally, the recent release of the experimentally solved structure of the complex between adenosine and the A2B receptor subtype,[37] allowed us to investigate also the binding mode of BRA1, despite not having any experimental data about the binding (Figure S12 and S13, Supporting Information). As for all previously discussed cases, docking results are compatible with the binding of BRA1 to the A2B binding site with a binding pattern superimposable to the one of adenosine. However, as adenosine itself shows less affinity for A2B compared to other subtypes (Table 1) and it has been demonstrated how this is related to the ECL2,[38] which is not experimentally solved in both A2B structures, it is tentative to speculate that BRA1 could also have less affinity for A2B compared to other receptor subtypes regardless of the congruence of the bound state.

Discussion

In the world of GPCRs, the 1:1 binding stoichiometry concerning the orthosteric site is a dogma that has yet to be experimentally challenged. Inspired by the pioneering computational work of Deganutti et al.,[9] which investigated the possibility of the adenosine receptor A2 A to contemporarily host two adenosine molecules within its orthosteric binding site, in the present scientific work we tried to address the issue by synthesizing a bis-ribosyl adenosine derivative (N6-(D-ribos-1-yl)-adenosine /BRA1), experimentally determining its binding affinity toward different adenosine receptor subtypes and computationally evaluating its interaction mode. Pharmacological assays elucidated that BRA1 is active against each considered receptor subtype (A1, A2 A, and A3, respectively), being able to bind and activate them with a potency in the range of low μM. The performed synthetic route led to a solution equilibrium between five different isomeric species of BRA1, that can be interconverted through the opening and closure of the secondary ribose unit ring.

To rationalize the activity profile of BRA1 and give structural insights into the possibility for the orthosteric binding site to contemporarily harbor two different ribose units, docking calculations were performed for each BRA1 isomer on each adenosine receptor subtype. Docking results indicate that BRA1 nicely fits within the orthosteric binding site of the receptor subtype with each of its solution forms. Among the various isomer, the α-ribofuranose isomer (α-FUR) is the one that is better able to reproduce the binding determinants of the endogenous ligand adenosine and seems, indeed, the most competent isomer for orthosteric site recognition. Despite the better interaction profile for α-FUR, other isomers are also able to fit within the orthosteric sites with a slightly worse interaction pattern compared to the reference adenosine which still retains most of the features required for the recognition of the endogenous agonist. This observation indicates that the activity of BRA1 against various adenosine receptor subtypes could be attributed to the cooperative effort portrayed by each of its equilibrium solution species rather than by a process that strictly involves one of the isomers.

Concerning the different affinity for each receptor subtype, the highest affinity of BRA1 for adenosine receptor A1 compared to the A2 A and A3 subtypes could be explained by the fact that A1 is the only case in which the bis-ribosyl adenosine derivative (particularly, the α-FUR isomer) is predicted to have a binding mode superimposable to that of adenosine, with the addition of some ulterior interactions with residue located in the upper portion of the binding site through the N6-linked ribose unit. This region, which involves three residues that are part of the second extracellular loop (ECL2) including the crucial phenylalanine residue involved in the π-stacking with the adenine core of adenosine, presents a diverse amino acid composition across different receptor subtypes, leading to a different predicted interaction pattern with the N6-linked ribose unit that could represent an additional explanation for the different binding affinity of BRA1 toward the different receptor species. Due to the peculiar location of these residues within the orthosteric site, situated at the entrance of the pocket in a region that is renowned for its importance in determining the binding specificity of GPCRs, the exploitation of techniques that go beyond the final bound state and

investigate the binding process in its integrity such as Supervised Molecular Dynamics will be needed to fully characterize and rationalize the role that these residues might play in the recognition process. Investigation in this sense is already going on within our laboratory and will be part of future scientific works.

Finally, the comparison between the computational analysis performed on BRA1 and recent works performed within our laboratory reveals two important aspects of the binding features of this bis-ribosyl derivative. The first aspect is that, contrary to expectations, the binding pattern of BRA1 is more similar to that described for non-ribose agonists rather than ribose ones,[34] due to the constraints posed on the position of the adenine core by the presence of the secondary ribose unit in the upper portion of the binding site. The second and most important implication, which is closely related to the first one, is that the binding determinants for the BRA1 compound are in agreement with observations on the ternary complex formed by two adenosine molecules in the work of Deganutti et al.,[9] with the loss of interaction with the asparagine residue located in the sixth transmembrane helix being compensated by the strengthening of other interactions and the addition of other ones mediated by the secondary ribose unit.

Conclusions

Taken altogether, all the observations made in the present study support the possibility of a 2:1 binding stoichiometry for the adenosine within the orthosteric binding site of adenosine receptors. Nevertheless, to fully disclose the importance of this region in discriminating the binding affinity and the binding pattern of BRA1, techniques that holistically analyze the binding event and not only focus on the final stage (i.e., the bound complex) such as Supervised Molecular Dynamics would be required and, as anticipated before, computational investigations in this sense are already going on within our laboratory and will be part of future scientific works.

The results of this work expand the knowledge on the process of ligand recognition by adenosine receptors, paving the way for the discovery of peculiar binding processes, and may be inspiring the design of novel active chemical entities that enlarge the pool of pharmacological tools available to target not only adenosine receptors but also other class A GPCRs.

Experimental Section

Experimental protocol

Adenosine (≥99%), D-(−)-ribose (95-98%), and all solvents were purchased from Merck. and have been used without further purification. TLC plates (aluminium back silica gel /UV 254, 0.25 mm) were purchased from Macherey Nagel and eluted using 3:1 EtOAc/CH3OH. Compounds were visualized using a 254-nm UV lamp or by staining with a solution of 1% KMnO4. Column chromatography was performed using Silica gel 60 as stationary phase (Merck, 230–400 ASTM mesh) and 3:1 EtOAc/CH3OH as mobile phase. The 1H NMR and two-dimensional 1H-1H COSY, HSQC, and TOCSY spectra were recorded with a 500 MHz Varian spectrometer using the signal of the residual protons of D2O as a reference (δ 4.61 at T = 40 °C). The ESI mass spectra were recorded with a Massa Esquire 4000-Bruker mass spectrometer which uses an electrospray ionization (ESI) source and an Ion-Trap analyzer. The accurate mass was obtained with a micrOTOF–Q-Bruker with an electrospray ionization (ESI) source and time of flight (TOF) analyzer for the analysis of accurate masses. The reactions were performed in a Monowave 400 Anton Paar high-performance microwave reactor or in a CEM Discovery Microwave Reactor. HPLC analysis was performed on an Agilent Infinity System 1260 chromatograph equipped with a quaternary pump (G1311CR), an analytical column C18 (Zorbax Eclipse Plus 3.5 μm 95 Å, Agilent 100×4.6 mm), and a wavelength UV detector variable (G1314BR). The elution conditions were: flow 1 mL/min, λ = 250 nm, injected volume 20 μL, solvent A H2O MilliQ, solvent B CH3CN. The elution gradient was: 0–5 min 0% B, 5–25 min 0–8% B, 25–30 min 8–0% B, 30–35 min 0% B. The LC/MS analysis was performed on an Agilent Infinity System 1260 chromatograph equipped with a quaternary pump (G1311B), a C18 analytical column (LUNA 5 μm 100 Å, 150×2 mm Phenomenex), a Photodiode Array Detector (G1312 C) and an LC/MS quadrupole (6120). The elution conditions were: flow 0.5 mL/min, injected volume 2 μL, solvent A H2O MilliQ + 0.1% HCOOH, solvent B CH3CN + 0.1% HCOOH. The elution gradient was: 0–5 min 0% B, 5–25 min 0–8% B, 25–30 min 8% B, 30–35 min 8–0% B. For HPLC and LC/MS analysis 2 mg of pure N6-(D-ribos-1-yl)-adenosine was dissolved in 1 mL of H2O MilliQ to obtain a 5 mM solution which was then diluted 1:10 (0.5 mM) in H2O MilliQ.

Synthesis of N6-(D-ribos-1-yl)adenosine

The substrates adenosine (150 mg, 0.56 mmol, 1 eq) and D-(−)-ribose (386 mg, 2.57 mmol, 4.6 eq) were suspended in 1 mL of anhydrous methanol (700 μL) and glacial acetic acid (300 μL) and the resulting suspension was irradiated in a microwave oven for 60 min at 100 °C, power 850 W, stirrer speed 800 rpm. The time course of the reaction was monitored by TLC analysis; Rf adenosine = 0.43, Rf N6-(D-ribos-1-yl)-adenosine = 0.17. At reaction completion, the resulting yellow solution was evaporated under vacuum, and the solid residue was solubilized in the minimum volume of CH3OH, applied on a silica gel column (2.50×17 cm), and eluted. The fractions containing the title product were pooled and evaporated to dryness under reduced pressure to give 135 mg of a very hygroscopic white solid (yield 60%). 1H NMR (500 MHz, 40 °C, D2O): D2O,): δ 8.35 (s, H8), 8.35 (s, H8), 8.34 (s, H8), 8.33 (s H2), 8.32 (s, H2), 8.30 (s, H2), 8.28 (s,H2), 6.16 (0.07H, br s, H1′′), 6.06 (1H, dd, J = 5.9, 1.3 Hz, H1′), 5.94 (0.05H, br d, H1′′), 5.68 (0.43H, br s, H1′′), 5.65 (0.43H, br d, H1′′), 4.76 (1H, q, J = 5.7 Hz, H2′), 4.41 (1H, m, H3′), 4.41 (m, H2′′), 4.33 (m, H3′′), 4.29 (m, H2′′), 4.29 (m, H3′′), 4.27 (1H, m, H4′), 4.09 (m, H3′′), 4.09 (m, H4′′), 4.09 (m, H4′′), 4.07 (m, H4′′), 4.05 (m, H2′′), 3.96 (m, H3′′), 3.93 (m, H5′′), 3.91 (m, H5′′), 3.90 (1H, m, H5′), 3.86 (m, H4′′), 3.85 (m, H5′′), 3.85 (m, H2′′), 3.83 (m, H5′′), 3.82 (1H, m, H5′), 3.76 (m, H5′′), 3.76 (m, H5′′), 3.75 (m, H5′′), 3.70 (m, H5′′). ESI-MS: m/z 400.2 [MH+]; 422.1 [M + Na+]. (+)-HRESI-TOFMS: m/z 422.1281 [M + Na+] (calcd for $C_{15}H_{21}N_5O_8Na$, 422.1282).

Computational part

Software overview

All the molecular modeling operations were executed with the Molecular Operating Environment (MOE) suite (version 2019.01).[11]

The preparation of the proteins downloaded from the Protein Data Bank (PDB[12]) was carried out using the dedicated tools of the MOE suite. The homology modeling operations necessary to create the virtual structure of human A3 receptors were also performed with the dedicated tool of the MOE suite. The operations necessary for the preparation of the ligands for molecular docking calculations were carried out with the tools of the QUACPAC package of the OpenEye[13] suite. For molecular docking calculations, the exploited program was Glide[14] (a systematic docking program developed and distributed commercially by Schrödinger). Both the modeling tasks and the docking runs have been executed on a 20 CPU Linux Workstation (Intel i9-9820X).

Protein preparation

To evaluate the binding mode of the N6-(D-ribos-1-yl)-adenosine derivative to the various human adenosine receptor subtypes, we chose as reference the experimental structures of the GPCRs under evaluation with the adenosine molecule crystallized within the orthosteric binding site.

Concerning the A1, A2 A, and A2B receptors, their three-dimensional structures were both retrieved from the Protein Data Bank (PDB). Particularly, the system with accession code 6D9H (method: Cryo-EM, resolution: 3.60 Å)[15] was chosen as a representative structure for the A1 receptor, the crystal with code 2YDO (method: X-ray crystallography, resolution: 3.00 Å)[16] was selected for A2 A receptor, while the structure 8HDP (method: Cryo-EM, resolution: 3.20 Å)[38] was selected for A2B.

Before any computational operation, the receptors have been aligned to their respective FASTA sequence, allowing to highlighting of the presence of mutated residues, that was reformulated with the Protein Builder application present in MOE. Then, both structures have been properly prepared for computational handling using the dedicated tools present in the MOE suite. Specifically, the Structure Preparation tool was exploited to rebuild the small missing loops in the structures, the Protonate 3D application was applied to assign to each residue the proper protonation state at pH 7.4, and finally, the added hydrogen atoms were energy minimized under the AMBER10:EHT force field implemented in MOE.[17] Due to the lack of experimental structure of the human A3 receptor to date, the complex between the adenosine and the A3 receptor was created through homology modeling, using as the template the A1 receptor previously prepared. This operation was performed with the appropriate tool implemented in the MOE suite. The choice of template was made based on a study previously published by our laboratory, which showed how models created on A1 perform better than models created using A2a as a template.[18] Furthermore, we avoided AlphaFold since it is biased toward inactive state structures,[19] while we are interested in investigating the adenosine receptors in the active state, the one induced by binding to the endogenous agonist adenosine.

Ligand preparation

N6-(D-ribos-1-yl)-adenosine presents a solution equilibrium that involves five different isomeric forms: the open-ring configuration, the α/β ribopyranose, and the α/β ribofuranose. Open-ring configuration aside, whose concentration is negligible (see Supporting Information), each other isomer was considered as a separate entity and investigated accordingly. For clarity reasons, the four species will be referred to as α-FUR (α-ribofuranose), β-FUR (β-ribofuranose), α-PYR (α-ribopyranose), and β-PYR (β-ribopyranose), respectively. Each aforementioned ligand was prepared for docking calculations using the tools of the QUACPAC package available in the OpenEye suite. Specifically, the tautomers tool was used to highlight the most appropriate tautomer for each ligand, the OMEGA application was exploited to generate the 3D coordinates of the molecules, and the MolCharge tool was then used to calculate the partial charges under the MMFF94 force field. Finally, the dominant protonation state at pH 7.4 was calculated using the FixpKa application.

Molecular docking

The four ligands, prepared as described above, were docked in the orthosteric binding pocket of A1, A2 A, A3, and A2B receptors using the Glide docking package. Specifically, a three-dimensional grid was centered upon the co-crystallized adenosine molecules for A1, A2 A, and A2B, while for A3 the same coordinates of A1 were kept, given the fact that the A3 model is based on A1. A radius of 15 Å was used to define the grid borders, and the default settings for grid generation were kept. After the grid generation, molecular docking calculations were carried out using Glide, with Glide-SP chosen as the scoring function, keeping all other parameters as default. For each of the four ligands of interest, 50 poses were generated, which were then filtered to eliminate the ones presenting steric clashes or unfavorable electrostatic interactions with the protein. The remaining poses were then analyzed by exploiting an in-house Python script that performs a per-residue interaction energy decomposition including a comparison with a reference pose. For each receptor subtype, the adenosine crystallographic pose was set as the reference pose. The script analyzes both the electrostatic interaction energy (expressed in Kcal/mol) and the strength of the hydrophobic contact (expressed in arbitrary units), plotting the final results as comparative per-residue heatmaps. For each ligand pose, an RMSD value (representing the congruency of the interaction pattern between the reference pose and the query) is calculated and reported. The most representative pose for each compound was then chosen according to the RMSD value (the lower, the better) and by visual inspection, fetching for poses that maintain the recognition features that are pivotal to the recognition of adenosine within the orthosteric binding site.

Pharmacological experiments

Cell culture and membrane preparation

Chinese Hamster Ovary (CHO) transfected with human (h) adenosine receptors (ARs) subtypes hA1, hA2 A, hA2B, and hA3 ARs (Perkin Elmer, Boston, MA, USA) were grown in adhesion in Dulbecco's modified Eagle's medium with nutrient mixture F12, supplemented with 10% fetal calf serum, penicillin (100 U/mL), streptomycin (100 μg/mL), L-glutamine (2 mM) and geneticine (G418; 0.2 mg/mL), at 37 °C, in a humified atmosphere with 5% CO2, until their use in cAMP assays.[20] Regarding membrane preparation to be used in competition binding experiments, cells were rinsed with phosphate-buffered saline and scraped off T75 flasks in ice-cold hypotonic buffer (5 mM Tris·HCl, 1 mM EDTA, pH 7.4) after the culture medium has been removed. The resulting suspension of cells was homogenized employing a Polytron and centrifuged for 30 min at 40,000× g, at 4 °C, to obtain the membrane pellet to be used for experiments.[21]

Competition binding experiments

The compound affinity to hA1, hA2 A, and hA3 ARs was examined. Competition binding experiments to hA1AR were performed incubating 2-chloro-*N*6-[^{3}H]cyclopentyladenosine ([^{3}H]CCPA) (1 nM)

with membrane suspension (50 μg of protein/100 μL) and different concentrations of the tested compound at 25 °C for 90 min in 50 mM Tris·HCl, pH 7.4. Non-specific binding was determined in the presence of 1 μM CCPA and was always < 10% of the total binding.[20]

Inhibition binding experiments to hA2 A ARs were carried out through the incubation of the radioligand [^{3}H]4-(−2-[7-amino-2-{2-furyl}{1,2,4}triazolo{2,3-*a*} {1,3,5}triazin-5-yl-amino]ethyl)phenol ([^{3}H]ZM241385) (1 nM) with the membrane suspension (50 μg of protein/100 μL) and different concentrations of the examined compound for 60 min, at 4 °C, in 50 mM Tris·HCl, 10 mM $MgCl_2$ (pH 7.4). Non-specific binding was defined with ZM241385 (1 μM) and was about 20% of the total binding. Moreover, hA2 A ARs competition binding experiments were also performed by using (2-[*p*-(2-carboxyethyl)phenethylamino]-5′-*N*-ethylcarboxamidoadenosine) ([^{3}H]CGS 21680) as radioligand (15 nM) incubated with the membrane suspension (50 μg of protein/100 μL) and different concentrations of the tested compound for 90 min at 25 °C in 50 mM Tris·HCl, 10 mM $MgCl_2$ (pH 7.4). Nonspecific binding was determined in the presence of CGS 21680 (1 μM) and was about 25% of the total binding.[22]

Inhibition binding assays to A3ARs were conducted by incubating the membrane suspension (50 μg of protein/100 μL) with 0.5 nM [^{125}I]*N*6-(4-aminobenzyl)-*N*-methylcarboxamidoadenosine ([^{125}I]ABMECA) in the presence of different concentrations of the examined compound for 120 min, at 4 °C, in 50 mM Tris·HCl, 10 mM $MgCl_2$, 1 mM EDTA (pH 7.4). Non-specific binding was defined as binding in the presence of 1 μM ABMECA and was always < 10% of the total binding.[21]

The bound radioactivity was separated from the free one by filtering the assay mixture through Whatman GF/B glass-fiber filters, using a Brandel cell harvester (Brandel Instruments, Unterföhring, Germany). The filter-bound radioactivity was counted by Packard Tri Carb 2810 TR scintillation counter (Perkin Elmer).

Cyclic AMP assays

CHO cells transfected with hA1, hA2 A, hA2B, and hA3 ARs were washed with phosphate-buffered saline, detached with trypsin, and centrifuged for 10 min at 200× g. Cells were seeded in a 96-well white half-area microplate (Perkin Elmer, Boston, USA) in a stimulation buffer composed of Hank Balanced Salt Solution, 5 mM HEPES, 0.5 mM Ro 20–1724, 0.1% BSA. For A1 and A3 ARs, different concentrations (1 nM–1 mM) of BRA1 were incubated for 30 min before the addition of 1 μM Forskolin for another 30 min to stimulate cAMP production. For A2 A and A2B ARs, cAMP levels were analysed after incubation of the cells with various concentrations (1 nM–1 mM) of BRA1 for 30 min. The cAMP levels were quantified utilizing the AlphaScreen cAMP Detection Kit (Perkin Elmer, Boston, MA, USA), according to the manufacturer's instructions.[23] Finally, the plate was read with a Perkin Elmer EnSight Multimode Plate Reader.

Data analysis

The protein concentration was determined using a Bio-Rad method, with bovine albumin as a standard reference. Inhibitory binding constant (Ki) values were calculated from those of IC50 according to the Cheng–Prusoff equation, Ki=IC50/(1 + [C*]/KD*), where [C*] is the concentration of the radioligand, and KD* its dissociation constant. Ki and IC50 or EC50 values were calculated by non-linear regression analysis, using the equation for a sigmoid concentration-response curve (Graph-PAD Prism, San Diego, CA, USA).

Acknowledgements

The MMS lab is very grateful to Chemical Computing Group, OpenEye, and Acellera for their scientific and technical partnership. The MMS lab gratefully acknowledges the support of NVIDIA Corporation with the donation of the Titan V GPU, used for this research.

Conflict of Interests

The authors declare no conflict of interest.

Data Availability Statement

The data that support the findings of this study are available on request from the corresponding author. The data are not publicly available due to privacy or ethical restrictions.

Keywords: adenosine receptors · adenosine · bis-ribosyl-adenosine · receptor recognition · receptor activation · bitopic ligands

[1] S. H. E. Kaufmann, *Nat. Rev. Drug Discovery* **2008**, *7*, 373–373.
[2] K. A. Berg, W. P. Clarke, *Int. J. Neuropsychopharmacol.* **2018**, *21*, 962–977.
[3] J. Liu, R. Nussinov, *PLoS Comput. Biol.* **2016**, *12*, e1004966.
[4] R. Hurst, H. Rollema, D. Bertrand, *Pharmacol. Ther.* **2013**, *137*, 22–54.
[5] S. B. Gacasan, D. L. Baker, A. L. Parrill, *AIMS Biophys.* **2017**, *4*, 491–527.
[6] N. R. Latorraca, A. J. Venkatakrishnan, R. O. Dror, *Chem. Rev.* **2017**, *117*, *139–155*.
[7] K. Leach, P. M. Sexton, A. Christopoulos, *Trends Pharmacol. Sci.* **2007**, *28*, 382–389.
[8] P. J. Conn, A. Christopoulos, C. W. Lindsley, *Nat. Rev. Drug Discovery* **2009**, *8*, 41–54.
[9] G. Deganutti, V. Salmaso, S. Moro, *Mol. Inf.* **2018**, *37*, 1800009.
[10] D. Sabbadin, S. Moro, *J. Chem. Inf. Model.* **2014**, *54*, 372–376.
[11] Molecular Operating Environment (MOE), 2019.01; Chemical Computing Group ULC, 1010 Sherbooke St. West, Suite #910, Montreal, QC, H3 A 2R7 (Canada), 2021.
[12] H. M. Berman, *Nucleic Acids Res.* **2000**, *28*, 235–242.
[13] QUACPAC 2.1.3.0: OpenEye Scientific Software, Santa Fe, NM. http://www.eyesopen.com.
[14] T. A. Halgren, R. B. Murphy, R. A. Friesner, H. S. Beard, L. L. Frye, W. T. Pollard, J. L. Banks, *J. Med. Chem.* **2004**, *47*, 1750–1759.
[15] C. J. Draper-Joyce, M. Khoshouei, D. M. Thal, Y. L. Liang, A. T. N. Nguyen, S. G. B. Furness, H. Venugopal, J. A. Baltos, J. M. Plitzko, R. Danev, W. Baumeister, L. T. May, D. Wootten, P. M. Sexton, A. Glukhova, A. Christopoulos, *Nature* **2018**, *558*, 559–563.
[16] G. Lebon, T. Warne, P. C. Edwards, K. Bennett, C. J. Langmead, A. G. Leslie, C. G. Tate, *Nature* **2011**, *474*, 521–525.
[17] D. A. Case, T. A. Darden, T. E. Cheatham, III, C. L. Simmerling, J. Wang, R. E. Duke, R. Luo, M. Crowley, R. C. Walker, W. Zhang, K. M. Merz, B. Wang, S. Hayik, A. Roitberg, G. Seabra, I. Kolossváry, K. F. Wong, F. Paesani, J. Vanicek, X. Wu, S. R. Brozell, T. Steinbrecher, H. Gohlke, L. Yang, C. Tan, J. Mongan, V. Hornak, G. Cui, D. H. Mathews, M. G. Seetin, C. Sagui, V. Babin, P. A. Kollman, **2008**, AMBER 10, University of California, San Francisco.
[18] E. Margiotta, S. Moro, *Appl. Sci.* **2019**, *9*, 821.
[19] A. Mullard, *Nat. Rev. Drug Discovery* **2021**, *20*, 725–727.
[20] F. Vincenzi, M. Targa, R. Romagnoli, S. Merighi, S. Gessi, P. G. Baraldi, P. A. Borea, K. Varani, *Neuropharmacology* **2014**, *81*, 6–14.
[21] D. Catarzi, F. Varano, E. Vigiani, S. Calenda, F. Melani, K. Varani, F. Vincenzi, S. Pasquini, N. Mennini, G. Nerli, D. Dal Ben, R. Volpini, V. Colotta, *Pharmaceuticals* **2022**, *15*, 478.

[22] F. Varano, D. Catarzi, F. Vincenzi, M. Betti, M. Falsini, A. Ravani, P. A. Borea, V. Colotta, K. Varani, *J. Med. Chem.* **2016**, *59*, 10564–10576.
[23] A. Ravani, F. Vincenzi, A. Bortoluzzi, M. Padovan, S. Pasquini, S. Gessi, S. Merighi, P. A. Borea, M. Govoni, K. Varani, *Int. J. Mol. Sci.* **2017**, *18*, 697.
[24] P. C. Jain, *Indian J. Chem.* **1968**, *11*, 616–618.
[25] N. E. Price, M. J. Catalano, S. Liu, Y. Wang, K. S. Gates, *Nucleic Acids Res.* **2015**, *43*, 3434–3441.
[26] M. Battistini, S. Mahajan, D. Diaz, L. Shaw, D. Merkler, *Curr. Microw. Chem.* **2016**, *3*, 124–130.
[27] C. Chavis, C. de Gourcy, F. Dumont, J.-L. Imbach, *Carbohydr. Res.* **1983**, *113*, 1–20.
[28] S. J. Cortes, T. L. Mega, R. L. Van Etten, *J. Org. Chem.* **1991**, *56*, 943–947.
[29] M. M. Quesada-Moreno, L. M. Azofra, J. R. Avilés-Moreno, I. Alkorta, J. Elguero, J. J. López-González, *J. Phys. Chem. B* **2013**, *117*, 14599–14614.
[30] M. Tomasz, R. Lipman, M. S. Lee, G. L. Verdine, K. Nakanishi, *Biochemistry* **1987**, *26*, 2010–2027.
[31] J. Fuentes Mota, M. A. Pradera Adrian, C. Ortiz Mellet, J. M. Garcia Fernandez, R. Babiano Caballero, J. A. Galbis Perez, *Carbohydr. Res.* **1988**, *173*, 1–16.
[32] B. B. Fredholm, E. Irenius, B. Kull, G. Schulte, *Biochem. Pharmacol.* **2001**, *61*, 443–448.
[33] A. Temeriusz, T. Gubica, P. Rogowska, K. Paradowska, M. K. Cyrański, *Carbohydr. Res.* **2006**, *341*, 2581–2590.
[34] G. Bolcato, M. Pavan, D. Bassani, M. Sturlese, S. Moro, *Biomed.* **2022**, *10*, 515.
[35] A. Cuzzolin, G. Deganutti, V. Salmaso, M. Sturlese, S. Moro, *ChemMedChem* **2018**, *13, 522–531*.
[36] A. Nicoli, A. Dunkel, T. Giorgino, C. De Graaf, A. Di Pizio, *J. Chem. Inf. Model.* **2022**, *62*, 511–522.
[37] E. De Filippo, S. Hinz, V. Pellizzari, G. Deganutti, A. El-Tayeb, G. Navarro, R. Franco, S. Moro, A. C. Schiedel, C. E. Müller, *Biochem. Pharmacol.* **2020**, *172*, 113718.
[38] H. Cai, Y. Xu, S. Guo, X. He, J. Sun, X. Li, C. Li, W. Yin, X. Cheng, H. Jiang, H. E. Xu, X. Xie, Y. Jiang, *Cell Discovery* **2022**, *8*, 1–4.

Manuscript received: February 23, 2023
Revised manuscript received: April 26, 2023
Accepted manuscript online: April 27, 2023
Version of record online: May 10, 2023